

# Tribological Performance of Self-lubricating Cast Al-5Cu-1Mg Nanocomposite Reinforced with Graphene Nano Sheets

Mohammad Alipour

\* alipourmo@tabrizu.ac.ir

Faculty of Mechanical engineering, Department of Materials Engineering, University of Tabriz, Iran

Received: October 2022

Revised: April 2023

Accepted: May 2023

DOI: 10.22068/ijmse.3003

**Abstract:** This study was undertaken to investigate the influence of graphene nano sheets on the structural characteristics and dry sliding wear behaviour of Al-5Cu-1Mg aluminium alloy. The optimum amount of GNPs for proper grain refining was selected as 0.5 wt.%. T6 heat treatment was applied for all specimens before wear testing. Significant improvements in wear properties were obtained with the addition of GNPs combined with T6 heat treatment. Dry sliding wear performance of the alloy was examined in normal atmospheric conditions. The experimental results showed that the T6 heat treatment considerably improved the resistance of Al-5Cu-1Mg aluminium alloy to the dry sliding wear. The results showed that dry sliding wear performance of without T6 microstructure specimens was a lower value than that of with T6 specimens.

**Keywords:** Aluminium alloys, Casting, Graphene nano sheets, T6 heat treatment, Dry sliding.

## 1. INTRODUCTION

Aluminum and its alloys are one of the most widely used materials in different industries, such as aerospace, automotive and defense. This is due to their superior physical and mechanical properties, such as light weight, high specific strength, high specific modulus, and low thermal expansion coefficient [1-3].

However, the wear behavior of aluminum alloys is not superior and few methods have been proposed in the past to improve the wear behavior of aluminum alloys. One method to reduce friction and consequently deterioration of material under wear condition is applying liquid or solid lubricants. However, in some cases, such as high vacuum environment, high-speed, high applied loads, and extremely low or high temperature conditions, liquid and grease type lubricants are impossible [4]. Another approach to enhance the wear performance of aluminum and aluminum alloys is by replacing the liquid and grease type lubricants with solid lubricant coatings. The coatings are applied on the surface of materials by depositing via chemical or physical vapor deposition techniques to form a solid lubricant layer [5, 6].

Metal matrix composites have many potential applications, because of the unique property combinations that can be achieved. Metal matrix composites have been developed to respond to the demand for materials with high specific strength,

stiffness, and wear resistance. Due to its high wear loss nature it will not be applicable for many tribological applications. AMCs can be reinforced with SiC, Al<sub>2</sub>O<sub>3</sub>, B<sub>4</sub>C, TiC, TiB<sub>2</sub>, MgO, TiO<sub>2</sub> and BN.

More specifically, the addition of carbon allotropes, such as Carbon Nano Tubes (CNTs) and graphene as reinforcement in metal matrices to improve the performance of materials has been a topic of interest over the last few years [7].

Therefore, the investigation of tribological and mechanical behavior of aluminum based materials is becoming increasingly important. The incorporation of a carbon allotropes to a relatively soft matrix alloy, commonly aluminium, improves the strength, creep performance, and wear resistance of the alloy.

By adding these nano carbonous materials into aluminum matrices one can synthesize selflubricating aluminum matrix composites due to superior lubricant nature of CNTs and graphene materials [8].

Graphene, considered as the mother of all graphitic materials, has the perfect 2-D lattice consisting of SP<sup>2</sup> bonded carbon atoms. Due to its very distinguished properties like high Young's modulus (1 TPa), high fracture strength (125 GPa), very high thermal conductivity (5000 W m<sup>-1</sup>K<sup>-1</sup>) and electron mobility (200,000 cm<sup>2</sup>V<sup>-1</sup>s<sup>-1</sup>), it is of particular interest in tribology. The wear mechanism in graphene is generally attributed to the breakage of in-plane bonds

between carbon atoms and shearing at the interface of graphene layers. The friction on graphene surface is proposed to be due to Van Der Waal's interactions. This present investigation aims to study the effects of graphene nano particles and heat treatment on the microstructure and dry sliding wear behavior of Al-4.5Cu-1Mg aluminum alloy.

The main object of the present study is to study the effect of graphene nano plates on the structure and the influence of the structural refining on the hardness and dry sliding wear behavior of Al-4.5 Cu-1Mg nanocomposite.

## 2. EXPERIMENTAL PROCEDURES

The materials used in this investigation were 99% pure aluminum powder with an average particle size of 45  $\mu\text{m}$  and graphene nanoplatelets with an average thickness of approximately 5 layer and an average diameter of 25  $\mu\text{m}$ . Fig. 1 shows the SEM micrographs of Al powder and graphene nanoplatelets. To produce nanocrystalline MMNCs, the reinforcements (graphene nanoplatelets with 0.1, 0.3, 0.5 and 1 wt.%) were dispersed in 99.5% anhydrous ethanol by ultrasonication. The aluminum powder and the reinforcement slurry were added to ball milling for 2 hours at 450 rpm using a Ball to Powder Ratio of 15:1. It is important to note that the initial particle sizes of aluminum powder was found to

be 45 micron. However, after 2 hours of milling, the particle size of powders decreases by milling process. In addition, the morphology of the aluminum powders after milling change to flaky shape. The graphene nanoplatelets distribute uniformly between flaky shape aluminum powders. The morphology and size of the powders after 2 hours of milling was investigated by SEM. Fig. 2 shows the SEM micrographs and EDS analysis of flaky shapes Al powders and graphene after 2 hours of milling.

The Al-5Cu-1Mg aluminium alloy ingots cut into small pieces and then placed into a graphite crucible. The graphite crucible was placed in an electrical resistance.

Melting of aluminium alloy was done by heating it to a temperature of  $\sim 750^\circ\text{C}$ . Then, stirring of Al alloy melt was accomplished for 10-15 minutes with the help of a mechanical stirrer to homogenise the uniform temperature throughout and adding up of pre-heated aluminum powder and graphene nanoplatelets composite with different wt.% in the metal melt. Nanocomposites specimens have been prepared with weight% of 0.1, 0.3, 0.5, 0.7 and 1 graphene nanoplatelets reinforcements.

After successful addition of nano reinforcement particles and uniform mixing throughout, the composite melt was poured into a permanent mold prepared according to ASTM B557M-10 standard, Fig. 3.

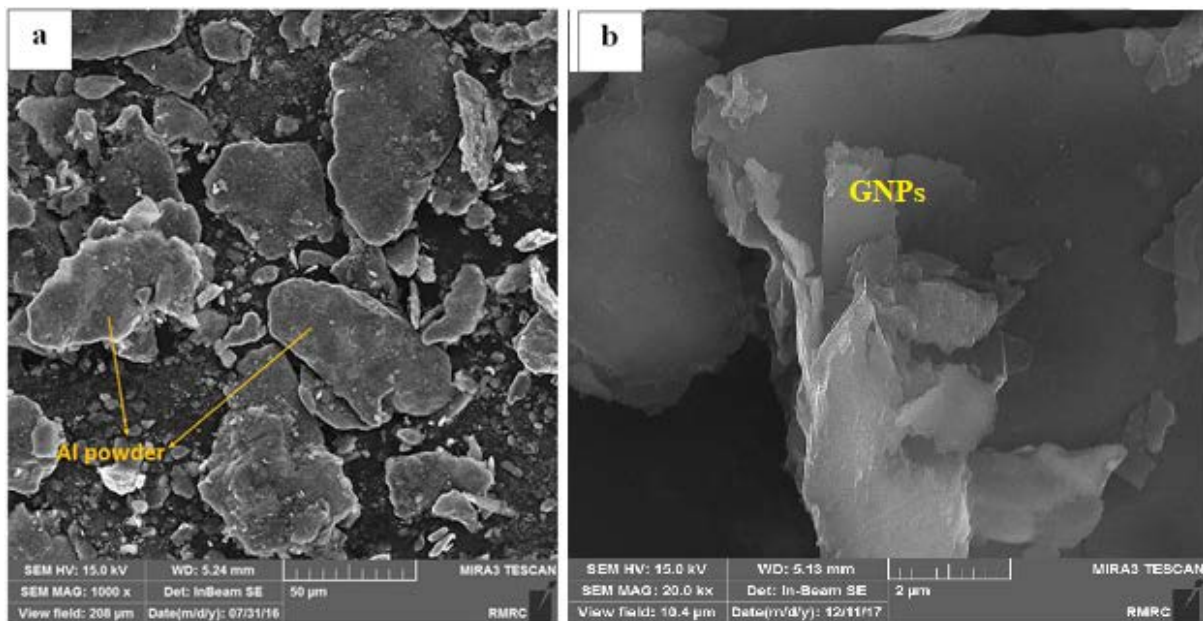


**Fig. 1.** SEM micrographs of a) and b) powder morphology of Al-25 wt% graphene nanoplatelets after 2 hours of milling.

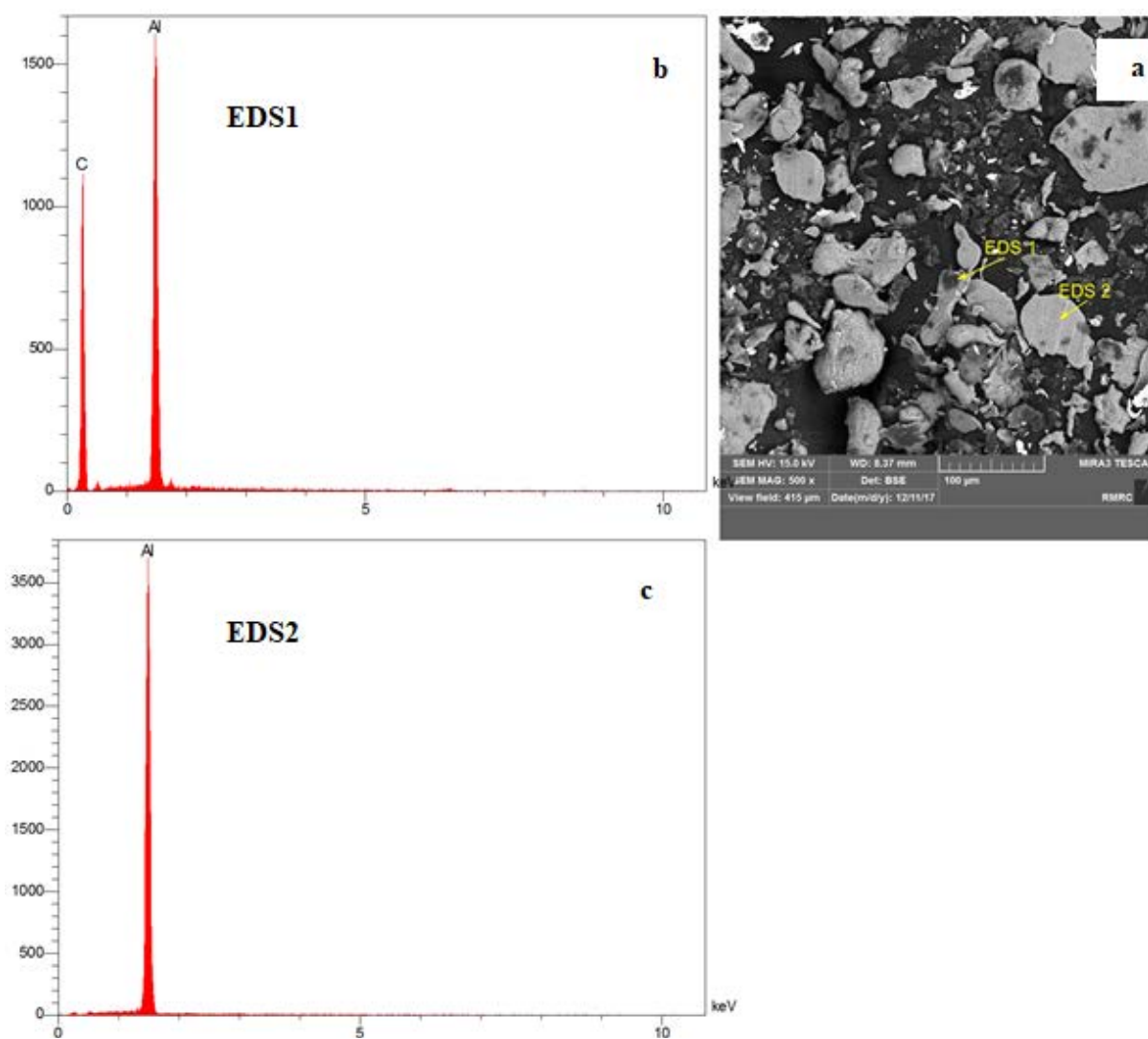


**Fig. 2.** Aluminum powder and graphene nano sheets, a) SEM image, b and c) elemental analysis of graphene nano sheets and aluminum particles.

The main advantage of this mold is the application of an appropriate uphill filling system and feeding design, providing a low turbulence manner of fluid flow, which results in reduced gas entrapment and porosity in the specimens.

Dry sliding wear tests were conducted using a conventional pin-on-disc testing machine to appraise room temperature (i.e., 25°C) wear behavior of the Al-5Cu-1Mg/graphene nanocomposite against a DIN 100Cr6 steel disk with a hardness of 62HRC. The pins 5 mm\* 20 mm, were in a conformal contact with the steel disk. Fig. 4 shows the schematic of the pin-on-disc configuration used in this study. The aluminum alloy was tested at a rotational speed of 250 rpm, corresponding to a speed of 0.5 ms<sup>-1</sup>, under nominal loads of 40 N and 20 N for a

sliding distance of 1500 m. The weight of the specimens was measured before and after the wear test using an electronic balance (GR200-AND) with an accuracy of 0.1 mg. For comparison, Al-5Cu-1Mg alloy and Al-5Cu-1Mg/graphene nanocomposite specimens were solutioned at 460°C for 8 h, quenched in water and artificially aged in 120°C for 24 h (T6 heat treatment), and structural studies and dry sliding wear behavior results were reported. [9]. Hardness test was carried out according to ASTM E10 standard using an Eseway tester (Brinell hardness: 30 kg force and indenter 2.5 mm). A comparison was made between the hardness results of the specimens prepared before and after T6 heat treatment. So, the specimens were solution treated at 460°C for 8 h, quenched in

water and artificially aged in 120°C for 24 h (T6 heat treatment).

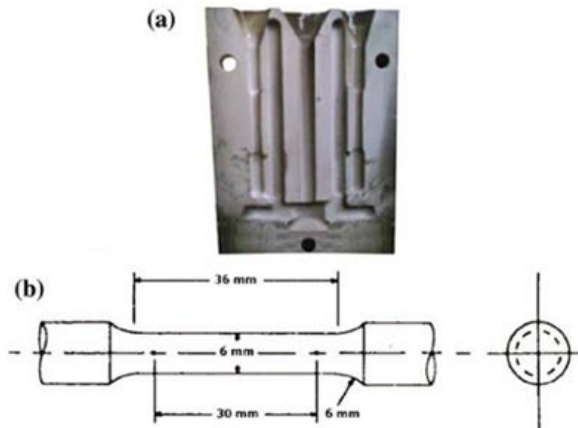


**Fig. 3.** a) Cast iron mold and b) tensile sample dimensions.

For structural studies, both an optical microscope equipped with an image analysis system (Clemex Vision Pro. Ver.3.5.025) and scanning electron microscope performed in a Cam Scan MV2300 scanning electron microscopy, equipped with an energy dispersive X-ray analysis (EDX) accessory have been used. The cut sections were polished and then etched by Keller's reagent (2 ml H, 3 ml HCl, 5 ml HNO<sub>3</sub> and 190 ml H<sub>2</sub>O) to reveal the structure. The average grain size of the specimens was measured according to the ASTM: E112 standard.



**Fig. 4.** Schematic of pin-on-disc configuration.

### 3. RESULTS AND DISCUSSION

#### 3.1. Structural Characterization

It is important to note that the initial particle sizes of aluminum powder was found to be 45 micron. However, after 2 hours of milling, the particle size of powders decreases by milling process, which can accommodate better dissolution and lower agglomeration during subsequent stir casting. In

addition, the morphology of the aluminum powders after milling change to flaky shape. Basically, the dissolution of small powders in the melt is easier than that of larger agglomerated ones. Two important events are responsible for formation of nanodispersions before solidification. First, the dissolution of aluminum powders during injection of powders into the melt. In fact, aluminum powders operate as a carrier for ceramic particles to the melt and protect them from any contact with the surface of the melt and alumina layer, and after their dissolution, the nanoparticles will be released in the matrix. Second, the power of ultrasonic vibration causes the agglomerated particles not being sintered. In fact, it is envisaged that aluminum powders which are in the inner part of an agglomerated nanoparticles act as a binder at 700°C to avoid particles separation and release, which only ultrasonic vibration could separate these nanoparticles during stirring.

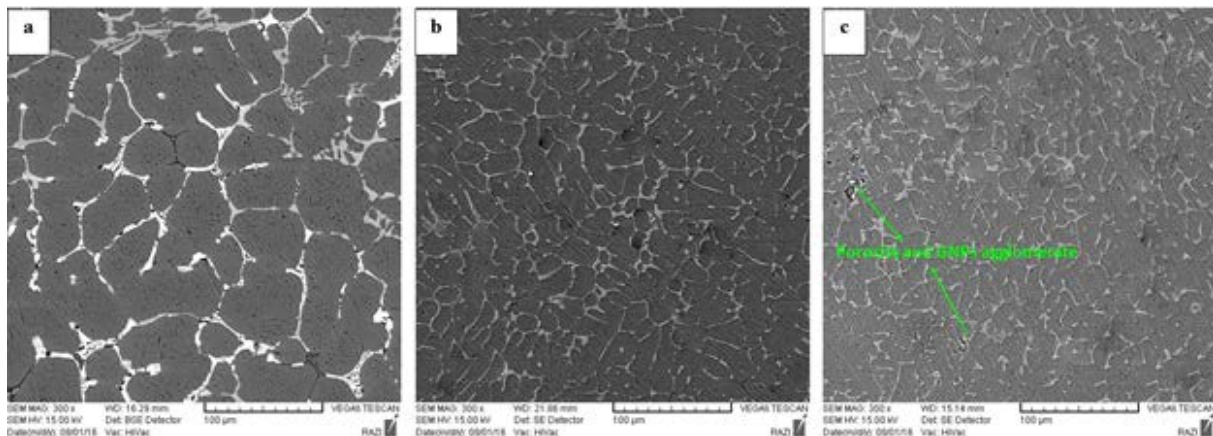
The microstructures of the Al-5Cu-1Mg alloy cut from castings after adding graphene with different percentage are shown in Fig. 5. Fig. 5 shows the change in dendrite morphology of the Al-5Cu-1Mg alloy after adding graphene. The optical microstructures of alloy revealed a rosette-like microstructure of primary  $\alpha$ -Al grains solid solution surrounded by interdendritic secondary phases. In comparison with graphene added specimens, unrefined specimens showed coarser morphology, as seen in Fig. 5. From Fig. 5, it is noticeable that graphene and stir casting enhances the number of grain boundaries and therefore promotes a more homogeneous distribution of intermetallic precipitates. The most common phase observed in as-cast microstructure in the Al-5Cu-1Mg alloys is Al<sub>2</sub>Cu ( $\theta$  phase). The optimum content of graphene nanoplates according grain size and mechanical properties is 0.5 wt%.

Fig. 6 shows the results from local analysis. The average composition of EDX analysis of the structure shows in Fig. 6. Fig. 6 shows the distribution of the major elements by scanning electron microscopy. Analysis of the EDX result of Al<sub>2</sub>Cu indicated that copper and aluminum contents are higher than the average level of chemical composition in the alloy. In spite of more contribution of aluminum, matrix may be involved in the EDX signal of the Al<sub>2</sub>Cu because of its small size. It is obvious that the Al<sub>2</sub>Cu

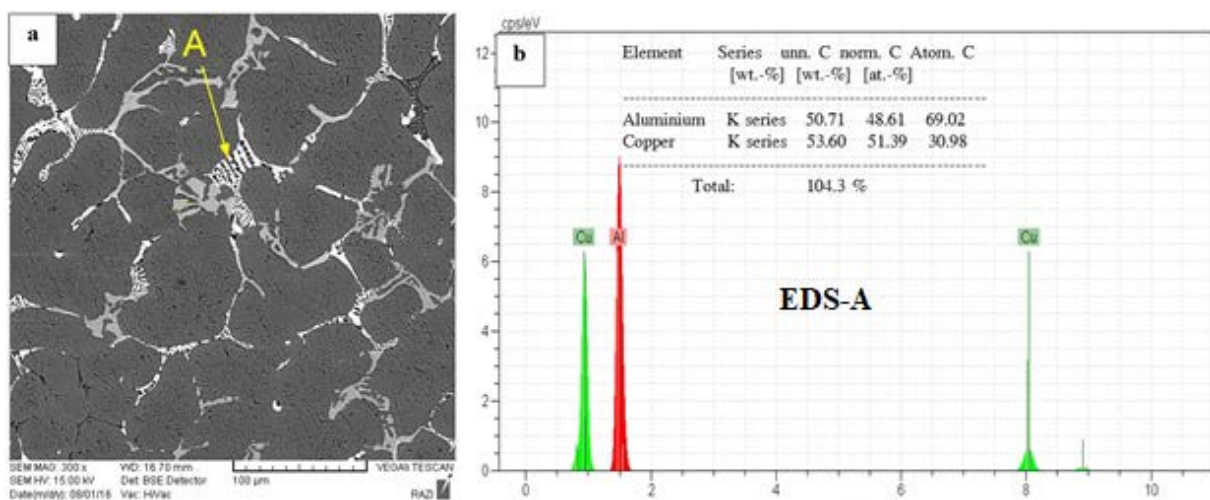
dissolved the Cu and Al elements which is consistent with the present literatures. The segregation of solute that occurred during casting led to the high concentration of Cu in the interdendritic regions.

Fig. 7 shows the distribution of graphene nanoplatelets in the Al-5Cu-1Mg aluminum alloy matrix in as-cast and 0.5 wt% after T6 heat treatment, the reinforcement particles are almost uniformly distributed in Al matrix, with graphene nanoplatelets content less than 1 weight%. As the graphene nanoplatelets content further increases, the agglomeration of graphene nanoplatelets occur. The clustering of graphene nanoplatelets increases markedly with 1 weight percentage of graphene nanoplatelets. Strengthening of these materials is due to the obstruction of dislocation movement by the graphene nanoplatelets. With increasing content of graphene nanoplatelets-these nanoplatelets pin the grain boundaries and

give rise to grain refinement, also nanoplatelets deflect cracks and cause increase of strength in nanocomposite. When weight % of graphene nanoplatelets is more than 0.5, the grain boundaries have reached saturation and effect of grain refinement diminished. Agglomeration of graphene nanoplatelets on the grain boundaries causes grain boundary embrittlement, porosity, resulting in weaker strength. It is clear from Fig. 5 that with the 1 weight % of graphene nanoplatelets, the nanoplatelets are forming clusters, grain boundary embrittlement, which create porosity, reduces the wettability of graphene nanoplatelets in the matrix materials and weakening of strength and other mechanical properties. It is important to note that the distribution of particles in aluminum matrix after T6 heat treatment were good and this condition causes high strength in specimens after T6 heat treatment.



**Fig. 5.** Microstructures of refined specimens, with a) 0.0% GNPs, b) 0.5% GNPs, c) 1% GNPs.



**Fig. 6.** a) Microstructures and EDX analysis of b)  $Al_2Cu$  ( $\theta$  phase) in unrefined specimens.

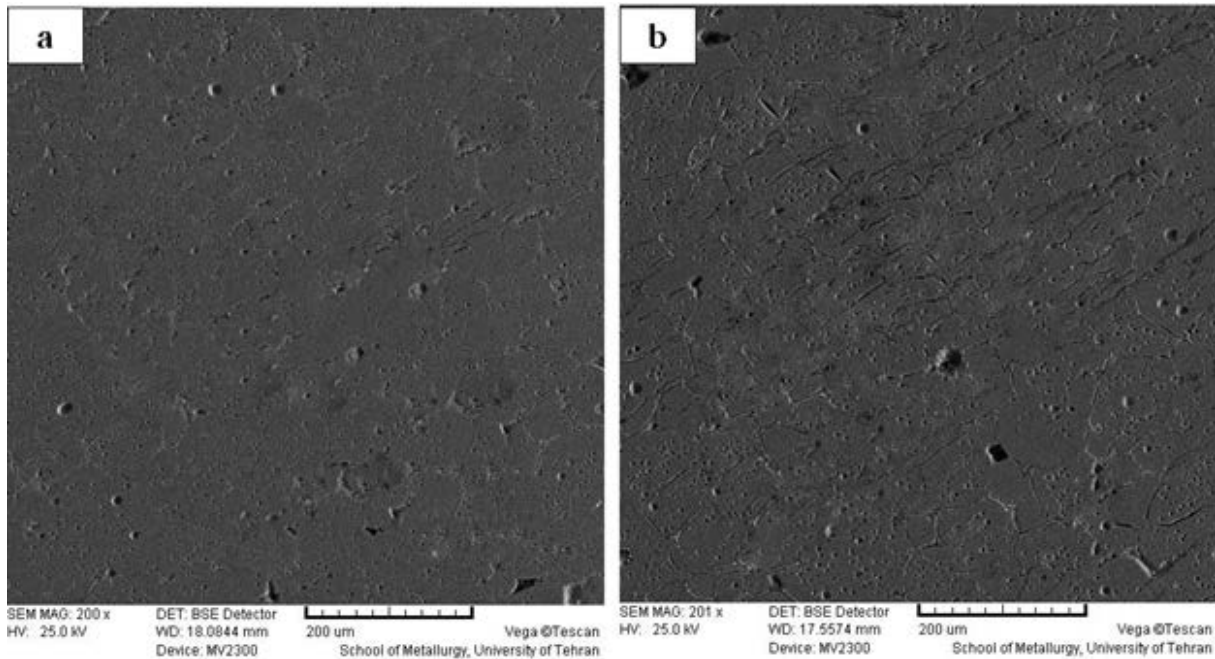


**Fig. 7.** SEM back-scattered images, showing the microstructures of the Al-5 Cu-1Mg alloy with: a) 0.0 and b) 0.5 wt% GNPs after T6 heat treatment.

### 3.2. Wear Behavior of Al-5Cu-1Mg/Graphene NanoPlate Nanocomposite

Fig. 8 shows the variation of coefficient of friction (COF) with normal load for Al-5Cu-1Mg aluminum alloy for unrefined and nanocomposite specimens with and without T6 heat treatment at constant sliding speed of 250 rpm.

The results indicate that the COF decreases with increasing normal loads in all cases. However, the rate of decrease in COF with normal load is significant at higher normal loads when compared to lower normal loads. The results show that the COF does not change significantly by adding 0.1 wt.% of GNPs to the aluminum matrix because of insufficient amount of solid lubricant available at the contact surface. However, higher weight percentage of GNPs (0.5 wt.%) decreased the COF of the composite sample significantly in comparison with other samples [10-12]

The wear results for Al-5Cu-1Mg aluminum alloy for unrefined and nanocomposite specimens with and without T6 heat treatment is shown in Fig. 9. Fig. 9 shows the amount of weight loss against sliding distance.

This diagram was obtained at constant normal loads (20 N and 40 N) and a constant rotation speed of the counter disk (250 rpm). It can be seen that the amount of weight loss has increased by

increase in sliding distance. Furthermore, increase in the amount of weight loss with sliding distance, approximately has a linear trend. Comparison between unrefined and nanocomposite specimens with and without T6 heat treatment for Al-5Cu-1Mg aluminum alloys is shown in Fig. 9.

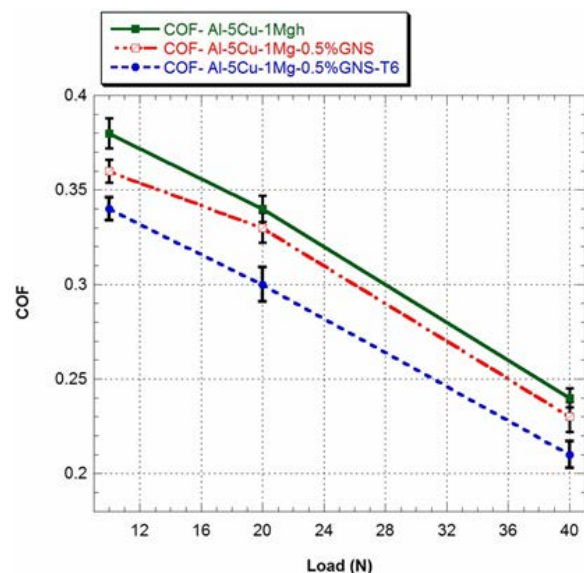


**Fig. 8.** COF values of the nanocomposite as function of load amount.

From Fig. 9, it is clear that the addition of graphene nano plate to Al-5Cu-1Mg aluminum

alloy has reduced the weight loss in comparison with unrefined aluminum alloy. This can be described in terms of uniform distribution and dispersion of graphene nano plate in refined by 0.5 %wt GNPs.

It is interesting to note that, the weight loss of the T6-tempered alloy, which was generally lower than those of untreated alloys in dry sliding wear tests. Probably due to the reduced grain size of the castings, leading to a finer distribution of second phases in Al-5Cu-1Mg-0.5GNPs-T6 nanocomposite. Wear surfaces of unrefined and nanocomposite specimens by 0.5 GNPs with and without T6 heat treatment are shown in Fig. 10. It can be seen a mild wear regime grooves the wear mechanism of the all alloys in Fig. 10. It clearly shows plastic deformation and delamination characteristics. Under an applied load of 40 N, two different regions are distinguished on the worn surface: cavities or craters and smooth regions marked as A and B in Fig. 10, respectively. In the smooth regions, the surface disclosed fine grooves and ploughing which suggest that abrasive wear was prevailing mechanism in these regions. Detached layer in the form of craters or cavities indicates locally adhesive wear due to the formation of and breaking of micro-welds during sliding. In addition, the wear rate of refined alloy by 0.5% GNPs with T6 heat treatment is lower than unrefined in all applied loads.

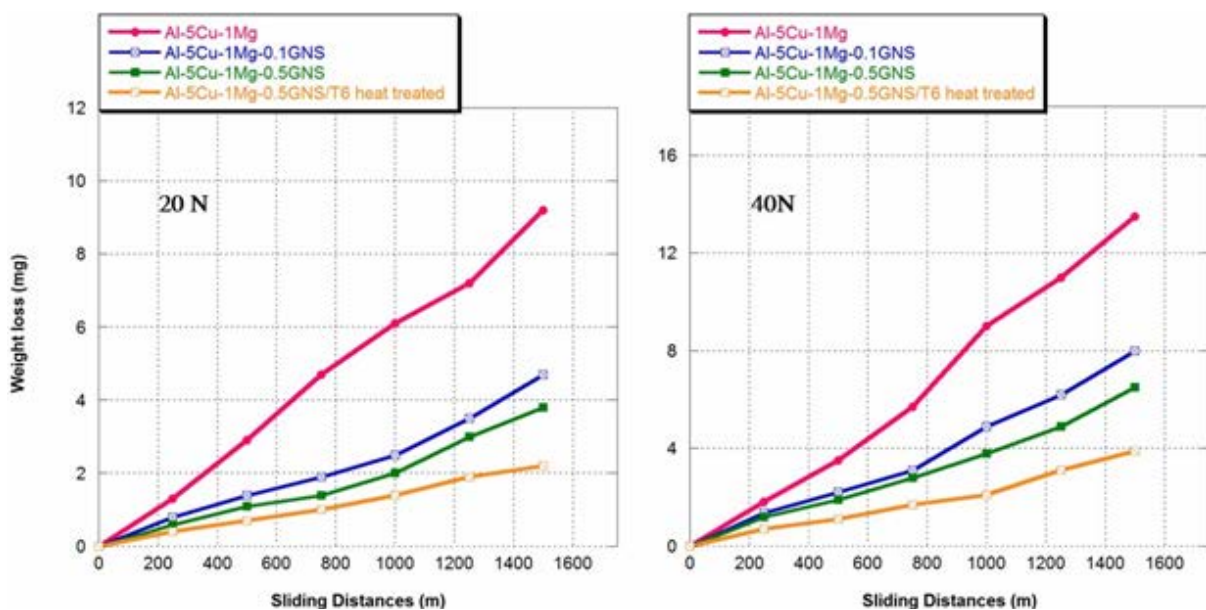
It seems that during the early stages of sliding, delamination wear is the dominant mechanism for the unrefined and nanocomposite specimens by 0.5% GNPs with and without T6 heat treatment. For unrefined Al-5Cu-1Mg aluminum alloys with coarse dendritic morphology can be easily broken and contribute to the weight loss [10].

Fig. 11 and 12 show SEM image and EDS analysis of the wear surface of nanocomposite reinforced with 0.5% by weight of graphene nanoplates under a force of 20 N after T6 heat treatment.

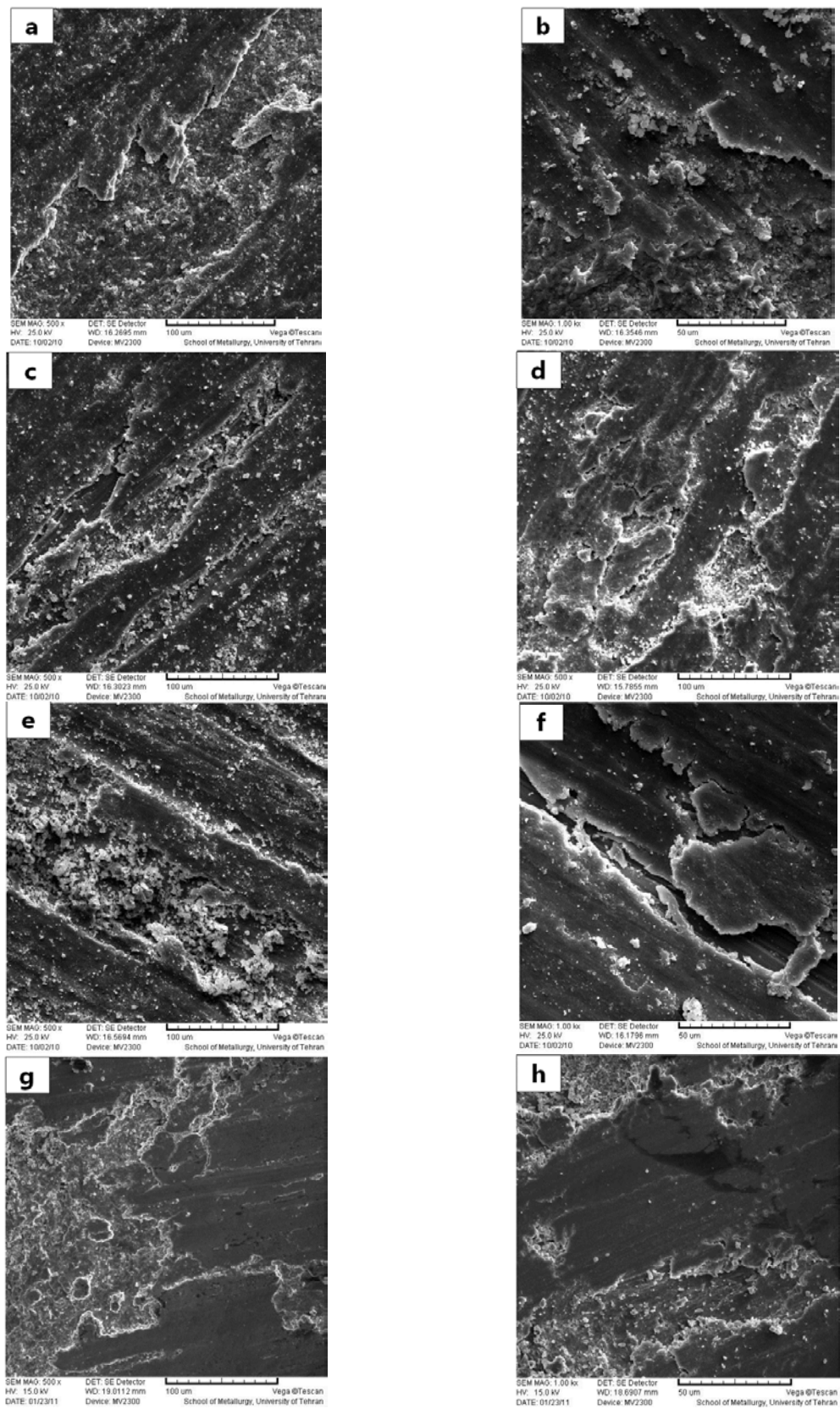
### 3.3. Hardness Results

Fig. 13 shows the hardness results of the specimens unrefined and nanocomposite specimens by 0.5% GNPs before and after solution and aging (T6 heat treatment). The slight improvement in hardness of the nanocomposite specimens could be a result of the effective dispersion of graphene nanoplates in matrix. Fig. 13 also shows that all specimens are sensitive to T6 heat treatment.

As expected, the hardness values of the nanocomposite specimens were found to be higher than those for the unrefined specimens. This may be due to the solid solution hardening of Al-5Cu-1Mg alloy by secondary solid elements at elevated holding time and temperature.



**Fig. 9.** Weight loss as a function of sliding distance for unrefined and refined nanocomposites with and without T6 heat treatment.



**Fig. 10.** Wear surface of the materials after 1500 m distance with 40 N load during wear process of a) and b) unrefined, c) and d) refined by 0.1 wt.% GNPs, e) and f) refined by 0.5 wt.% GNPs, g) and h) refined by 0.5 wt.% GNPs after T6 heat treatment.

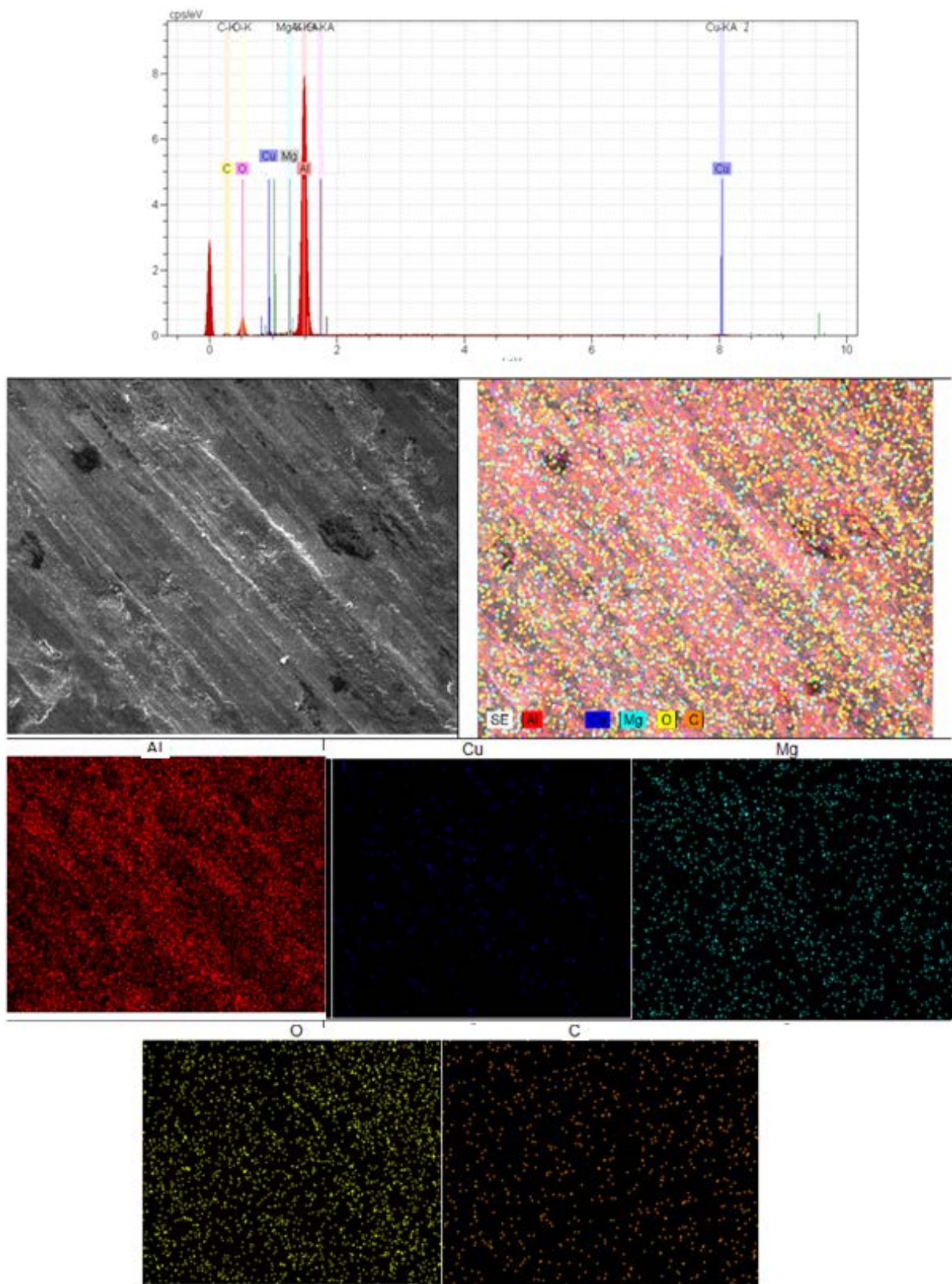


**Fig. 11.** SEM image and EDS analysis of the wear surface of nanocomposite reinforced with 0.5% by weight of graphene nanoplates under a force of 20 N after T6 heat treatment.

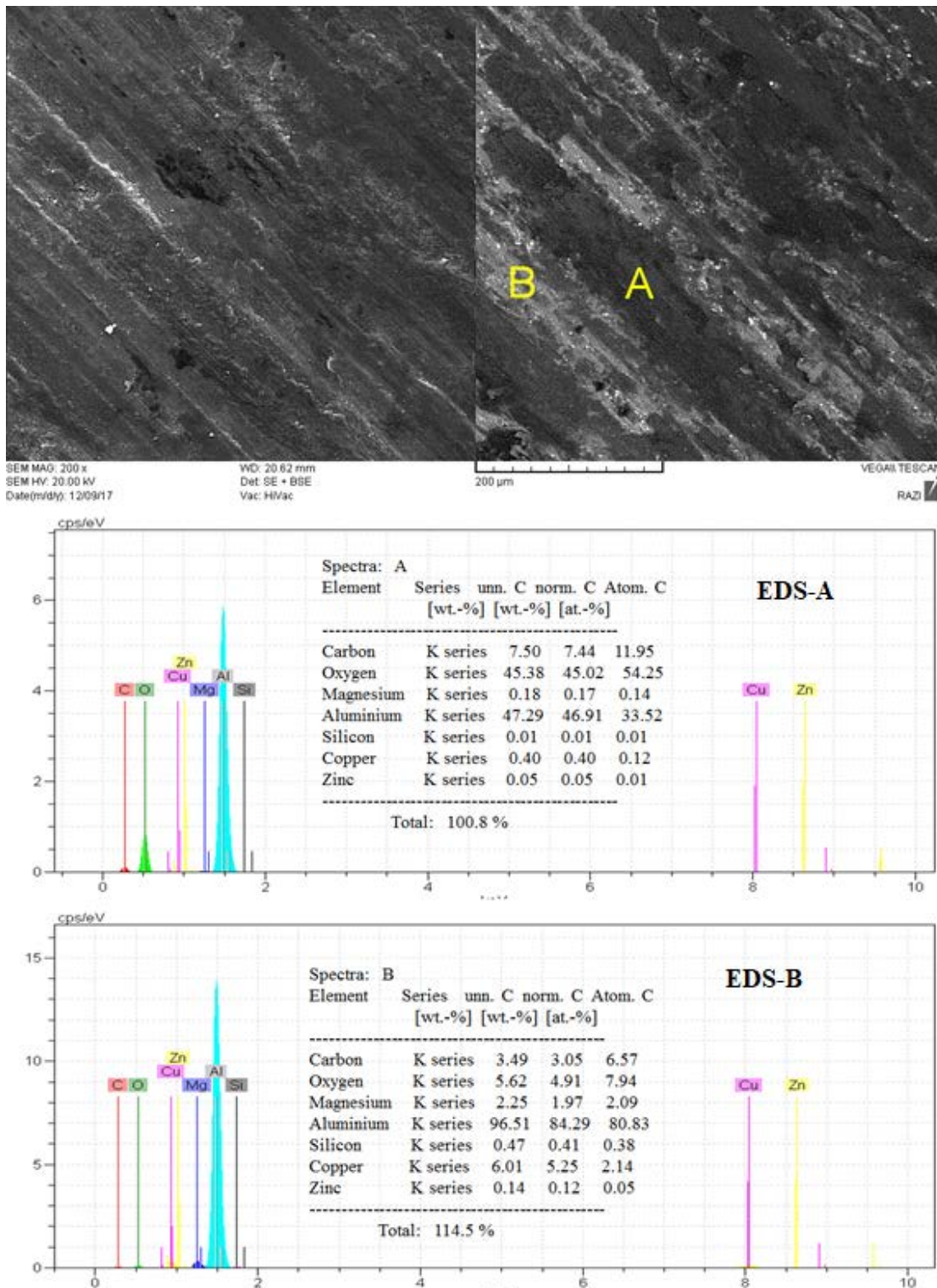


Fig. 12. The results of the EDS analysis of the wear surface of the nanocomposite sample containing 0.5 % GNPs by weight of graphene nanoplates after T6 heat treatment under a force of 20 N.

#### 4. CONCLUSIONS

In this study, Al-5Cu-1Mg matrix nanocomposites reinforced by GNP was

synthesized and the tribological behavior of these composites was investigated. The experimental findings are summarized as follows:

- The COF of the Al-5Cu-1Mg alloy and

Al-5Cu-1Mg matrix nanocomposites reinforced by GNP decreases with increasing the normal load.

- Addition of 0.1 wt.% of GNP to the Al-5Cu-1Mg matrix did not change the COF significantly when compared to the Al-5Cu-1Mg sample. However, the increasing amount of GNP to 0.5 wt% significantly improved the COF of the Al-5Cu-1Mg alloy.
- Among the all materials, namely, Al-5Cu-1Mg alloy, Al-5Cu-1Mg-0.1 wt.% GNP nanocomposite, Al-5Cu-1Mg-0.3 wt.% GNP nanocomposite, Al-5Cu-1Mg-0.5 wt.% GNP and Al-5Cu-1Mg-1 wt.% GNP nanocomposite, the Al-0.5 wt.% GNP nanocomposite recorded the lowest COF.
- The wear rate of the Al-5Cu-1Mg alloy and Al-5Cu-1Mg matrix nanocomposites reinforced by GNP increased with increasing the normal load.
- The wear rate of the Al-5Cu-1Mg alloy and Al-5Cu-1Mg matrix nanocomposites reinforced by GNP decreased with T6 heat treatment.
- The SEM investigation of the worn surfaces had shown that abrasive wear was the main wear mechanism in these composites.
- The lowest wear rate and coefficient of friction of the Al-0.5 wt.% GNP is attributed to self-lubricating behavior of the nanocomposites.

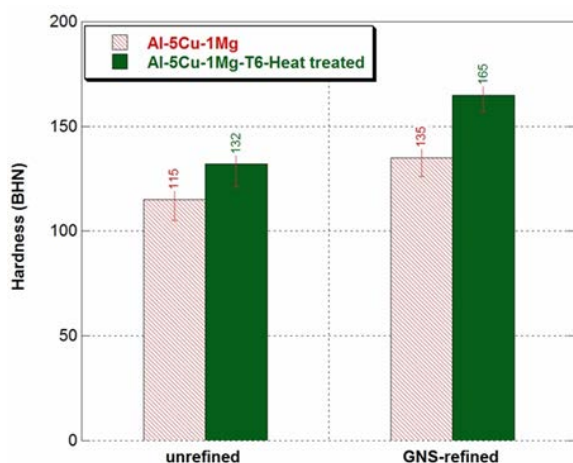


Fig. 13. Hardness of samples for unrefined and refined by 0.5 wt.% GNSs.

## REFERENCES

- [1]. Alipour, M., Emany, M., "Effects of Al-5Ti-1B on the structure and hardness of a

super high strength aluminum alloy produced by strain-induced melt activation process." *Materials & Design*, 2011, 32, 4485-4492.

- [2]. Alipour, M., Aghdam, B.G., Rahnoma, H.E., Emany, M., "Investigation of the effect of Al-5Ti-1B grain refiner on dry sliding wear behavior of an Al-Zn-Mg-Cu alloy formed by strain-induced melt activation." *Materials & Design*, 2013, 46, 766-775.
- [3]. Alipour, M., Azarbarmas, M., Heydari, F., Hoghoughi, M., Alidoost, M., Emany, M., "The effect of Al-8B grain refiner and heat treatment conditions on the microstructure, mechanical properties and dry sliding wear behavior of an Al-12Zn-3Mg-2.5Cu aluminum alloy." *Materials & Design*, 2012, 38, 64-73.
- [4]. Tjong, S.C., "Recent progress in the development and properties of novel metal matrix nanocomposites reinforced with carbon nanotubes and grapheme nanosheets." *Mater. Sci. Eng. R Rep*, 2013, 74, 281-350.
- [5]. Donnet, C., Erdemir, A., "Historical developments and new trends in tribological and solid lubricant coatings." *Surf. Coat. Technol*, 2004, 180-181, 76-84.
- [6]. Donnet, C., Erdemir, A., "Solid lubricant coatings: recent developments and future trends." *Tribol. Lett*, 2004, 17, 389-397.
- [7]. Moghadam, A., Omrani, E., Menezes, P.L., Rohatgi, P.K., "Mechanical and tribological properties of self-lubricating metal matrix nanocomposites reinforced by carbon nanotubes (CNTs) and graphene – a review." *Compos. Part B Eng*, 2015, 77, 402-420.
- [8]. Dorri Moghadam, A., Schultz, B.F., Ferguson, J.B., Omrani, E., Rohatgi, P.K., Gupta, N., "Functional metal matrix composites: self-lubricating, self-healing, and nanocomposites-an outlook." *JOM*, 2014, 66, 872-881.
- [9]. Haghparast, A., Nourimotlagh, M., Alipour, M., "Effect of the strain-induced melt activation (SIMA) process on the tensile properties of a new developed super high strength aluminum alloy modified by Al-5Ti-1B grain refiner." *Materials*

- Characterization, 2012, 71, 6-18.
- [10]. Alipour, M., Eslami-Farsani, R., “Synthesis and characterization of graphene nanoplatelets reinforced AA7068 matrix nanocomposites produced by liquid metallurgy route.” *Materials Science and Engineering A*, 2017, 706, 71-82.
- [11]. Mirjavadi, S. S., Alipour, M., Hamouda, A. M. S., Kord, S., Koppad, P. G., Abuzin, Y. A., Keshavamurthy, R., “Effect of hot extrusion and T6 heat treatment on microstructure and mechanical properties of Al-10Zn-3.5Mg-2.5Cu nanocomposite reinforced with graphene nanoplatelets.” *Journal of Manufacturing Processes*, 2018, 36, 264-271.
- [12]. Mirjavadi, S. S., Alipour, M., Hamouda, A. M. S., Matin, A., Kord, S., Mohasel Afshari, B., Koppad, P. G., “Effect of multi-pass friction stir processing on the microstructure, mechanical and wear properties of AA5083/ZrO<sub>2</sub> nanocomposites.” *Journal of Alloys and Compounds*, 2017, 726, 1262-1273.